Chiralities of spiral waves and their transitions

Jun-ting Pan,[1,*] Mei-chun Cai,[1,*] Bing-wei Li,[2,1,†] and Hong Zhang[1,‡]

[1]*Zhejiang Institute of Modern Physics and Department of Physics, Zhejiang University, Hangzhou 310027, China*
[2]*Department of Physics, Hangzhou Normal University, Hangzhou 310036, China*

The chiralities of spiral waves usually refer to their rotation directions (the turning orientations of the spiral temporal movements as time elapses) and their curl directions (the winding orientations of the spiral spatial geometrical structures themselves). Traditionally, they are the same as each other. Namely, they are both clockwise or both counterclockwise. Moreover, the chiralities are determined by the topological charges of spiral waves, and thus they are conserved quantities. After the inwardly propagating spirals were experimentally observed, the relationship between the chiralities and the one between the chiralities and the topological charges are no longer preserved. The chiralities thus become more complex than ever before. As a result, there is now a desire to further study them. In this paper, the chiralities and their transition properties for all kinds of spiral waves are systemically studied in the framework of the complex Ginzburg-Landau equation, and the general relationships both between the chiralities and between the chiralities and the topological charges are obtained. The investigation of some other models, such as the FitzHugh-Nagumo model, the nonuniform Oregonator model, the modified standard model, etc., is also discussed for comparison.

I. INTRODUCTION

A rotating vortex, the so-called spiral wave, can emerge from many different natural systems, such as cardiac muscle [1], the oxidation of CO on platinum [2], the Belousov-Zhabotinsky (BZ) reaction [3], etc. Due to its close relevance particularly to dangerous heart diseases, such as tachycardia and fibrillation [4–9], it is attracting much attention at present. The global dynamic behavior of a spiral is very complex, while some features can be well described by the motion of its rotation center. Usually, the center is defined by a phase singularity, which can be described in terms of the topological charge, or the winding number. And such topological charge is all the time a conserved quantity [10–13]. Owing to the conservation of the topological charge, there are some special dynamic properties for spiral waves. For example, the topological charges for the generated or annihilated spiral pair must be opposite; local changes for the concentrations of the reagents can make the phase singularity move but cannot destroy it, etc.

Traditionally, the topological charge can explicitly determine the chiralities of spiral waves, namely, their rotation directions (the turning orientations of the spiral temporal movements as time elapses) and their curl directions (the winding orientations of the spiral spatial geometrical structures themselves). Specifically, if it is positive, the rotation and the curl directions of spiral waves are both clockwise (CW), while if it is negative, they are both counterclockwise (CCW) [14]. That is, these two chiralities are the same as each other. Furthermore, the chiralities are conserved quantities being the same as the topological charge.

In general, these characteristics of chiralities serve well for spirals in uniform excitable media, where only outwardly propagating spirals (OPSs) exist. The inwardly propagating spirals (IPSs) were first observed in the oscillatory BZ reaction dispersed in water droplets of a water-in-oil microemulsion [15]. Since then, they have also been discovered in some other systems, such as the single-phase reaction-diffusion (RD) system [16], the artificial tissue of oscillatory cells [17], oscillatory glycolysis [18], etc., and have been extensively studied (see, e.g., Refs. [19–23]). In particular, they have also been observed numerically in nonuniform excitable media recently [24]. Now, the relationship between the rotation and the curl directions and the one between the chiralities and the topological charges, which work well for OPSs in uniform excitable media, are not preserved any more. The chiralities thus become more complex than ever before. Therefore, there is a desired need to further study them. In Ref. [25], the authors demonstrated that, generated from the same initial condition but with different system parameters in the perturbed complex Ginzburg-Landau equation (CGLE), the curl directions of spiral waves may be different. The authors in Ref. [26] illustrated that, during spiral transitions in the CGLE, the curl direction is conserved, but the rotation one is not conserved any more, while, the study in Ref. [27] showed that the curl direction is no longer conserved in the coupled CGLE (CCGLE) during spiral transitions, and the rotation one is still conserved in such processes. Now some natural problems are, more generally, whether the chiralities are still conserved, whether the topological charge is still conserved, and what are the essential relationships between the chiralities and the topological charges, especially, between the chiralities themselves?

This paper is aimed at systemically studying the general relationships both between the chiralities and the topological charges and between the chiralities themselves, and also at systemically studying the transition of the chiralities. For this purpose and for simplicity, we start our study with the simulation of the CGLE to investigate the properties for the chiralities and their transitions. At the same time, we

---

*J.T.P. and M.C.C. contributed equally to this work.
†Corresponding author: bwli@hznu.edu.cn
‡Corresponding author: hongzhang@zju.edu.cn

explore the general relationships between the chiralities and the topological charges and between the chiralities themselves. And we also analyze the conservation or nonconservation characteristics for the chiralities and also the topological charges. Then for comparison, we further investigate some other models, such as the FitzHugh-Nagumo (FHN) model, the nonuniform Oregonator model, the modified standard model, etc.

II. TOPOLOGICAL CHARGE AND CHIRALITIES

We now consider the following CGLE [28–30]:

$$\frac{\partial A}{\partial t} = (1 - i\omega)A - (1 + i\alpha)|A|^2 A + (1 + i\beta)\nabla^2 A, \quad (1)$$

where $A(x, y, t)$ is a complex field and describes the amplitude of the pattern modulations. The real parameters α and β are the nonlinear frequency shift and dissipative coefficient, respectively, and ω the linear frequency. ∇^2 denotes the two-dimensional Laplacian operator. This equation provides a universal description for spatially extended systems where their homogeneous states are oscillatory and in the vicinity of the supercritical Hopf bifurcation.

The topological charge of the spiral in the CGLE can be defined by [31]

$$W = \frac{1}{2\pi} \oint_\Gamma \nabla\phi \cdot \mathbf{dl} = \pm 1, \quad (2)$$

where $\phi = \arg A$, and Γ is a closed curve around the phase singularity where $A = 0$.

Following the methods in Refs. [14,32], it can be proved that

$$W = \text{sgn}[D(A/x)_{\text{PS}}], \quad (3)$$

where $D(A/x)$ is the z component of $\nabla A_1 \times \nabla A_2$; i.e., $D(A/x) = (\nabla A_1 \times \nabla A_2)_z$, with $A_1 = \text{Re}[A]$, and $A_2 = \text{Im}[A]$ being the real and the imaginary part of the complex field A, respectively. So,

$$D(A/x) = \left(\frac{\partial A_1}{\partial x} \frac{\partial A_2}{\partial y} - \frac{\partial A_1}{\partial y} \frac{\partial A_2}{\partial x} \right), \quad (4)$$

and $D(A/x)_{\text{PS}}$ is the value of $D(A/x)$ at the phase singularity. For a spiral, $|\nabla A_1 \times \nabla A_2|$ takes its maximum value approximately at the phase singularity, while it is almost zero in other regions. We can thus approximately identify the phase singularity position for a spiral by maximizing the value of $|\nabla A_1 \times \nabla A_2|$ [33].

Moreover, based on the same methods in Refs. [14,32], it can also be proved that W is a conserved quantity. Here, it is worth noting that the above discussions [including Eqs. (2) and (3)] are not limited to any specific type of spirals, so W is conserved for all kinds of spirals, including both OPSs and IPSs.

To study the spiral chiralities, we will numerically simulate the CGLE in the following. In the simulations, no-flux conditions are imposed at the boundaries, and the spiral waves are generated by the same cross-field initial condition in the different studied cases. The fourth-order Runge-Kutta algorithm is used for the integration, and the five-point approximation is chosen to discretize the Laplace operator.
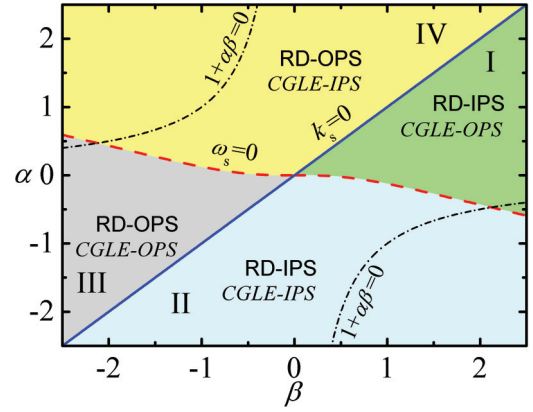

FIG. 1. (Color online) Parameter space (α, β) of the CGLE and four subdomains, I, II, III, IV, where OPS or IPS solutions exist in the CGLE and in the corresponding RD systems [21,22]. Here, $\omega = 0$.

And the space and the time steps are $\Delta x = \Delta y = 0.5$, and $\Delta t = 0.0125$, respectively.

The simulation shows that, with different parameters of α and β in the CGLE (see Fig. 1), there are four different forms of spiral waves as shown in Fig. 2. First of all and without loss of generality, we say that the curl direction in Figs. 2(a) or 2(c) is CCW (C^+, or $C = +1$. Here and hereafter, C is the shortened form of the curl direction), and the one in Figs. 2(b) or 2(d) is CW (C^-, or $C = -1$). We can see from Figs. 2(a) and 2(b) that, spirals with C^+ and C^- geometrical structures can both have an outward propagation (P^+, or $P = +1$. Here and hereafter, P is the shortened form of the propagation direction) direction; i.e., they are OPSs. And we can see from Figs. 2(c) and 2(d) that they can also both own an inward propagation (P^-, or $P = -1$) direction; namely, they are IPSs. That is, spirals with the same propagation directions may have opposite curl directions. At the same time, we can further see from Figs. 2(a) and 2(c), or from Figs. 2(b) and 2(d), that spirals with opposite propagation directions may have the same curl directions.

Moreover, we can get from Figs. 2(a) and 2(b) that spirals with a CCW rotation (R^+, or $R = +1$; here, R is the shortened form of the rotation direction, and hereafter) and a CW rotation (R^-, or $R = -1$) direction can be both OPSs, and from Figs. 2(c) and 2(d) that they can also be both IPSs. Namely, spirals with the same propagation directions may have opposite rotation directions. Meanwhile, we can also see from Figs. 2(a) and 2(d), or from Figs. 2(b) and 2(c), that spirals with opposite propagation directions may have the same rotation directions.

In addition, we can get from Figs. 2(a) and 2(d) that spirals with C^+ and C^- geometrical structures can both have a R^+ direction, and from Figs. 2(b) and 2(c) that they can also both have a R^- direction. Namely, spirals with the same rotation directions may have opposite curl directions. Besides, we can see from Figs. 2(a) and 2(c), or from Figs. 2(b) and 2(d), that spirals with opposite rotation directions may have the same curl directions.

As a whole, the above results show that the curl and the rotation direction are not always the same as each other. While here we must remember that all the above spirals are generated by the same initial condition, so their topological charges must be the same in principle. Indeed by calculating the value of $D(A/x)_{\text{PS}}$, we find in such all cases that its signs
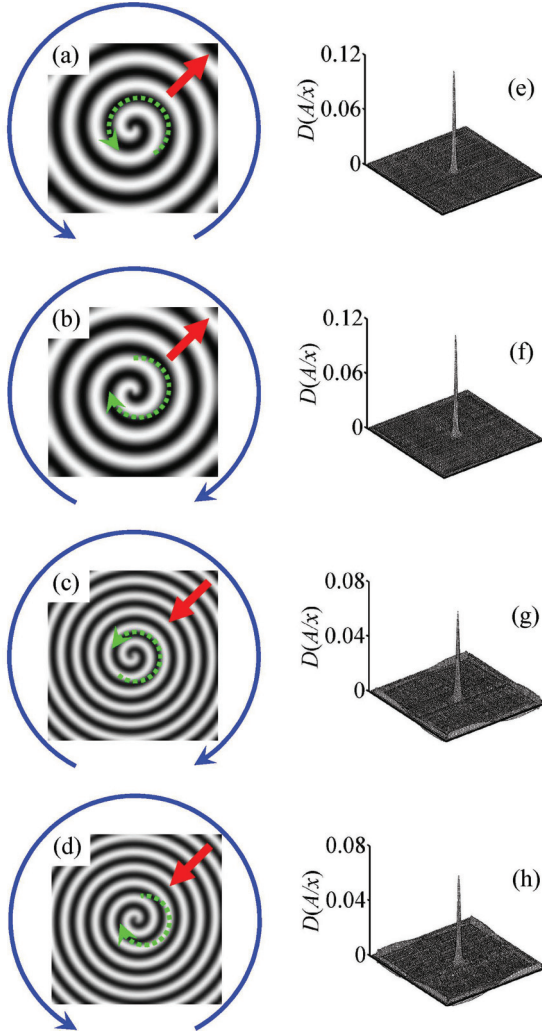
FIG. 2. (Color online) Four different forms of spiral waves for different parameters of α and β in the CGLE. (a) $\alpha = 0.17$, $\beta = 1.7$ (i.e., in subdomain I in Fig. 1); (b) $\alpha = -0.17$, $\beta = -1.7$ (i.e., in subdomain III in Fig. 1); (c) $\alpha = -0.34$, $\beta = 1.7$ (i.e., in subdomain II in Fig. 1); and (d) $\alpha = 0.34$, $\beta = -1.7$ (i.e., in subdomain IV in Fig. 1). In all four cases, $\omega = 0$. (e)–(h) Plots of $D(A/x)$ correspond one to one to cases (a)–(d). The system consists of 360×360 grid points. The solid curved arrow denotes the rotation direction of the spiral wave, and the dashed one represents its curl direction. The straight arrow denotes its propagation direction, here and hereafter.

stay the same as shown in Figs. 2(e)–2(h) or, for simplicity, in Table I [$D(A/x)_{PS} > 0$; i.e., the topological charge W is positive ($W = +1$)] regardless of the curl, the rotation, and the propagation directions of the spirals.
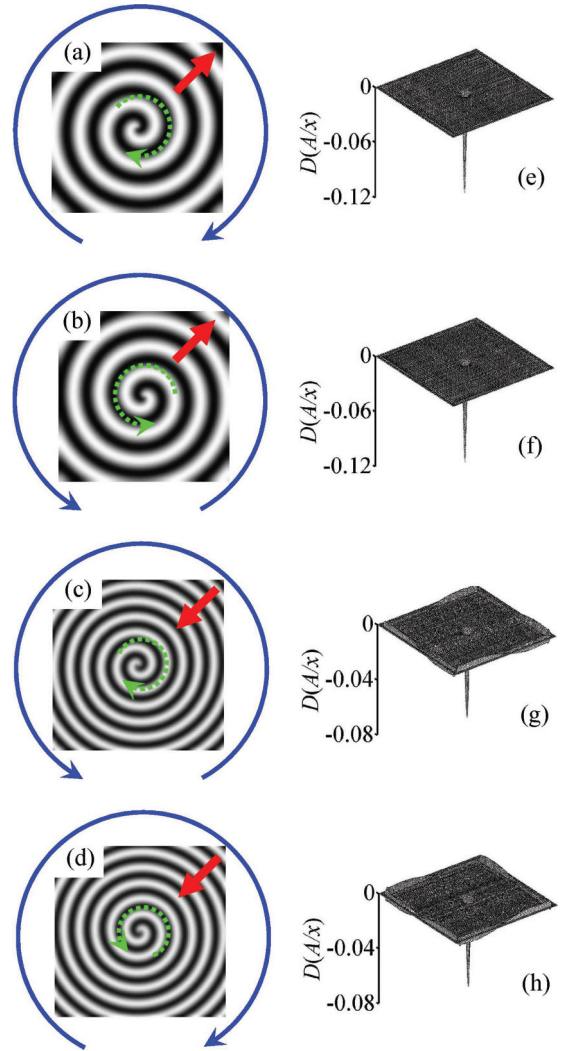
FIG. 3. (Color online) Four different forms of spiral waves in the CGLE. The parameters from (a) to (d) are the same as those in Fig. 2 correspondingly except for the initial condition. (e)–(h) Same meanings as those in Fig. 2.

By the careful analysis for the characteristics of the chiralities and the topological charge (e.g., see Table I), we further find that there is a fixed relationship between them, namely,

$$C \cdot R \cdot P = W. \tag{5}$$

Actually, when the topological charge W is negative ($W = -1$), we can also make a similar analysis in the same way as above. In this case, we can get from Fig. 3 or Table II that the

TABLE I. The chiralities of four types of spirals in the CGLE (the topological charge $W = +1$).

Curl	Rotation	Propagation	Topological charge	Spiral
$C = +1$	$R = +1$	$P = +1$	$W = +1$	Fig. 2(a)
$C = -1$	$R = -1$	$P = +1$	$W = +1$	Fig. 2(b)
$C = +1$	$R = -1$	$P = -1$	$W = +1$	Fig. 2(c)
$C = -1$	$R = +1$	$P = -1$	$W = +1$	Fig. 2(d)

TABLE II. The chiralities of four types of spirals in the CGLE (the topological charge $W = -1$).

Curl	Rotation	Propagation	Topological charge	Spiral
$C = -1$	$R = -1$	$P = +1$	$W = -1$	Fig. 3(a)
$C = +1$	$R = +1$	$P = +1$	$W = -1$	Fig. 3(b)
$C = -1$	$R = +1$	$P = -1$	$W = -1$	Fig. 3(c)
$C = +1$	$R = -1$	$P = -1$	$W = -1$	Fig. 3(d)

relationship between the chiralities and the topological charge will change to

$$C \cdot R \cdot P = -W. \tag{6}$$

Combining Eqs. (5) with (6), we can get the following relationship between the chiralities:

$$C \cdot R = P. \tag{7}$$

Note that, for spirals in uniform excitable media, there are only two cases: $(C,R,P,W) = (-1,-1,+1,+1)$ and $(C,R,P,W) = (+1,+1,+1,-1)$, which correspond to Figs. 2(b) and 3(b), respectively. And the relationship between the chiralities and the topological charges is greatly simplified: $C = R = -W$.

III. TRANSITIONS OF CHIRALITIES

To study the chirality transitions, for simplicity, we further numerically simulate the CGLE in the following. In the simulations, we use the same algorithm and its parameters as discussed in Sec. II. For convenience, the initial condition we use here is the well-developed spiral wave in Fig. 2(a), and we will study its transitions under the parameters in Figs. 2(b)–2(d).

By the simulations, we find when we change the parameters in Fig. 2(a) to the other ones in Figs. 2(b)–2(d), the original spiral in Fig. 2(a) will gradually and smoothly change its state to the other spirals in Figs. 2(b)–2(d) correspondingly (see Figs. 4, 6, and 7). Specifically, during the transitions between
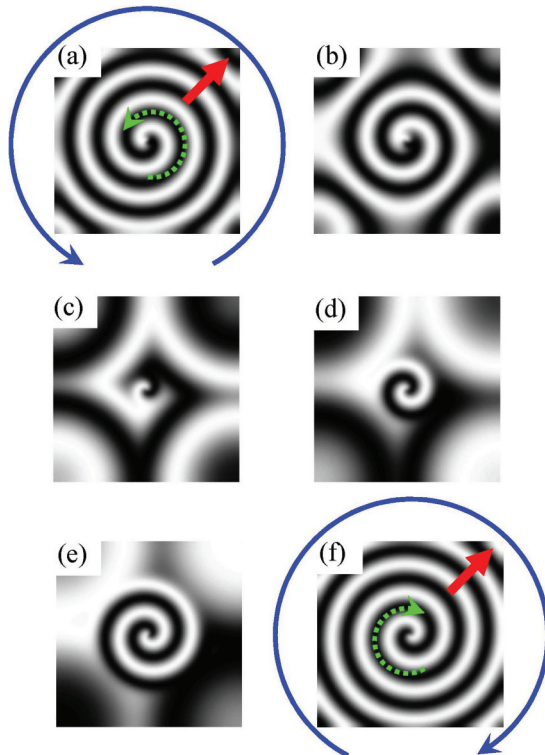

FIG. 4. (Color online) The transition of spiral wave from Figs. 2(a) to 2(b). $\alpha = -0.17$, $\beta = -1.7$, and $\omega = 0$. Snapshots are taken at (a) $t = 5.0$, (b) $t = 50.0$, (c) $t = 200.0$, (d) $t = 300.0$, (e) $t = 400.0$, and (f) $t = 675.0$.
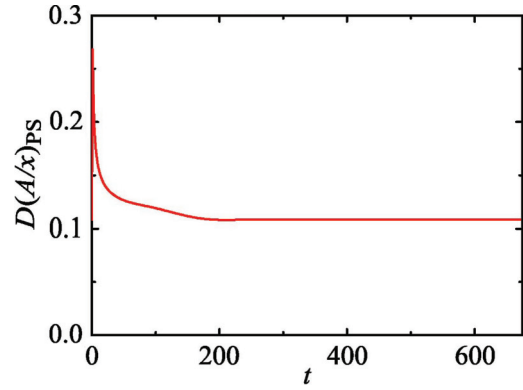

FIG. 5. (Color online) $D\,(A/x)_{\mathrm{PS}}$ in the CGLE during the spiral transition shown in Fig. 4. According to Eq. (3), $D\,(A/x)_{\mathrm{PS}} > 0$ gives the topological charge $W = +1$. The unchanging state of $D\,(A/x)_{\mathrm{PS}} > 0$ means that $W = +1$ stays the same. Namely, the topological charge W is conserved during the transition.

the spirals with different curl directions, the wave structure of the original spiral will deform greatly in the beginning, then its tip will suffer from a splitting effect resulting in an opposite orientation for the generation of the new spiral tip (see Figs. 4 and 7). And in the process of the transitions between the spirals with the same curl directions, the wave structure of the original spiral will not deform at first, and the new spiral tip directly generates from the original one in the same orientation free from the split (see Fig. 6). Moreover, the topological charge is of course conserved at all times regardless of the transition kinds (e.g., see Fig. 5).

The above results show that the spiral in Fig. 2(a) can change its state to any one of the three other spirals in Figs. 2(b)–2(d). Of course, the similar transitions can also be observed if we set any one of them as the original state in turn. This means that the chiralities of spiral waves are no longer conserved during
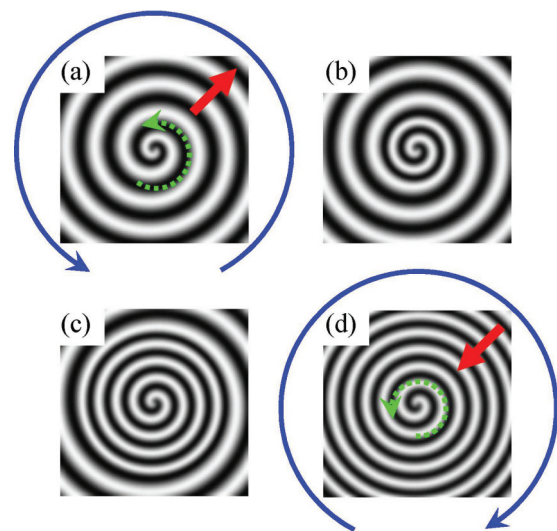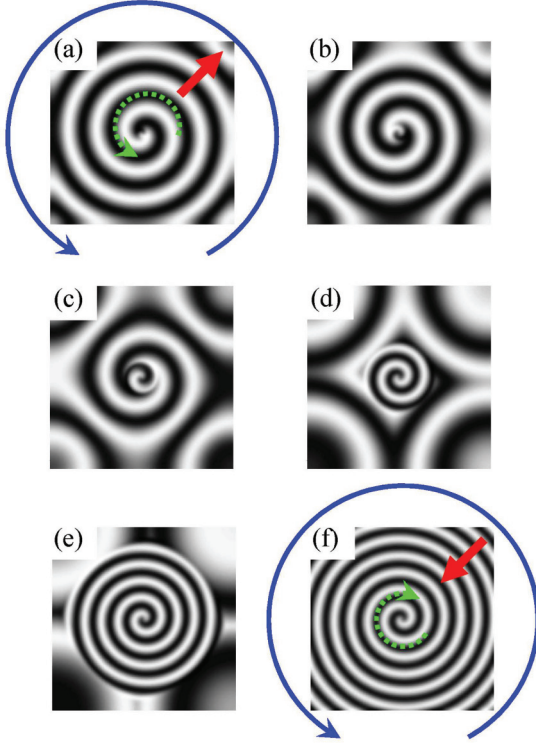

FIG. 6. (Color online) The transition of spiral wave from Figs. 2(a) to 2(c). $\alpha = -0.34$, $\beta = 1.7$, and $\omega = 0$. Snapshots are taken at (a) $t = 10.0$, (b) $t = 25.0$, (c) $t = 55.0$, and (d) $t = 90.0$. $D\,(A/x)_{\mathrm{PS}}$ is calculated, and $D\,(A/x)_{\mathrm{PS}} > 0$ holds over time; i.e., the topological charge W is conserved during the transition.

FIG. 7. (Color online) The transition of spiral wave from Figs. 2(a) to 2(d). $\alpha = 0.34$, $\beta = -1.7$, and $\omega = 0$. Snapshots are taken at (a) $t = 5.0$, (b) $t = 25.0$, (c) $t = 50.0$, (d) $t = 100.0$, (e) $t = 175.0$, and (f) $t = 250.0$. $D(A/x)_{PS}$ is calculated, and $D(A/x)_{PS} > 0$ stays unchanged as time elapses. That is, the topological charge W is conserved during the transition.

these transitions. Not only can each of the rotation and the curl direction change alone (see Figs. 6 and 7), but also both of them may change at the same time (see Fig. 4). And the same results can also be obtained if we consider the $W = -1$ case as shown in Fig. 3 or Table II. Meanwhile, we can see conveniently from Tables I or II that, in each case of the transitions, one of the three directions, i.e., C, R and P, can be survived, while the two others will have to be changed. Therefore, we can see that Eqs. (5)–(7) can work well during spiral transitions.
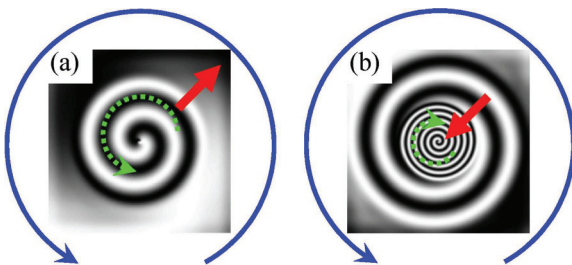

FIG. 8. (Color online) The transition of spiral wave from (a) to (b) in the CCGLE [27]: $\partial_t A = (1 - i\omega)A - (1 + i\alpha)|A|^2 A + (1 + i\beta)\nabla^2 A + K(z - A)$, and $\tau \partial_t z = A - z + l^2 \nabla^2 z$. z denotes the additional complex-valued diffusive field. The parameters are $K = 0.4$, $\tau = 10.0$, $l = 10.0$, $\omega = 0$; and (a) $\alpha = 0.7$, $\beta = -0.4$; (b) $\alpha = 0.9$, $\beta = -0.4$. $D(A/x)_{PS}$ is calculated, and $D(A/x)_{PS} > 0$ remains the same as time elapses. That is, the topological charge W is conserved during the transition.

TABLE III. The chirality transition in the CCGLE and the NCGLE. Here, Figs. 8(b) and 9(b) mean the newly formed spirals in their central parts.

Curl	Rotation	Propagation	Topological charge	CCGLE	NCGLE
$C = +1$	$R = +1$	$P = +1$	$W = +1$	Fig. 8(a)	Fig. 9(a)
$C = -1$	$R = +1$	$P = -1$	$W = +1$	Fig. 8(b)	Fig. 9(b)

Moreover, we find the above spiral transitions can also be observed in some other systems. As a case in point, we would like to study the CCGLE, one investigated in Ref. [27] recently. With suitable parameters, we can get the similar transition for spiral waves and their evolution properties as discussed in Ref. [27] (see Fig. 8). After this, we further examine the topological charge and find that it is conserved in such transition. We can see from Table III that, after the spiral transition, the curl direction is changed from $C = +1$ to $C = -1$, and the rotation direction stays the same, which is similar to that in Ref. [27] [see the spiral transition from Figs. 3(a) to 3(c) in Ref. [27]]. Equations (5) and (7) still work effectively because the propagation direction has been changed from $P = +1$ to $P = -1$ at the same time.

We also study the nonuniform CGLE (NCGLE) [34]. For simplicity, we use the well-developed spiral wave in Fig. 2(a) as the initial condition, and consider its evolution under the influence of disk-shaped inhomogeneity. The simulation shows that, if the original spiral in Fig. 2(a) suffers from the inhomogeneity effects, it will evolve into the so-called sink spiral as discussed in Ref. [34] (see Fig. 9). In this case, we also examine the topological charge and find that it is conserved. During the spiral transition, we also find, similar to the case of the CCGLE, that the chiralities are not conserved, and Eqs. (5) and (7) work well (see Table III).

Actually, as for the RD systems, the above spiral transitions in the uniform CGLE can also be reproduced except in the case of Fig. 6. The reason for this is that, as shown in Fig. 1, the two subdomains discussed in Fig. 6 (I and II) support two different
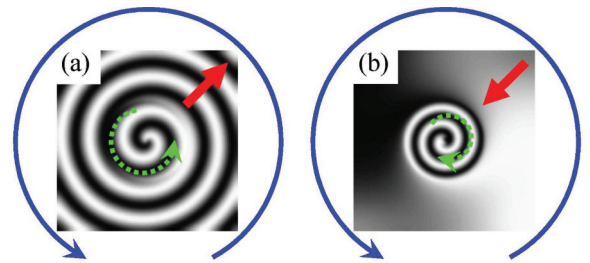

FIG. 9. (Color online) The sink spiral (b) generated from the spiral wave in Fig. 2(a) for the NCGLE [34]. Similar to Ref. [34], we consider ω in Eq. (1) to be a spatial function: $\omega(r) = 0$ for $r > R$, and $\omega(r) = \Delta\omega$ for $r \leqslant R$, where $r = \sqrt{(x - x_c)^2 + (y - y_c)^2}$ and (x_c, y_c) represents the center of the studied medium. The parameters are $R = 80.0$ and $\Delta\omega = -0.28$. Snapshots are taken at (a) $t = 5.0$ and (b) $t = 540.0$ after the original spiral in Fig. 2(a) suffered initially from the inhomogeneity effects. $D(A/x)_{PS}$ is calculated, and $D(A/x)_{PS} > 0$ remains unchanged as time passes. Namely, the topological charge W is conserved during the transition.

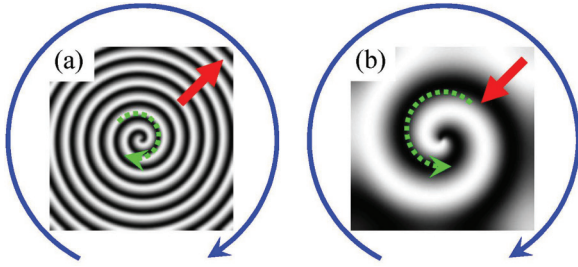FIG. 10. (Color online) The transition of spiral wave from (a) to (b) in the FHN model [22,34]: $\partial_t u = u - u^3/3 - v + D_u\nabla^2 u$, and $\partial_t v = \epsilon(u - \gamma v + \eta) + D_v\nabla^2 v$. u and v are the activator and the inhibitor variable, respectively. The parameters are $\gamma = 0.5$, $D_u = D_v = 0.005$. And (a) $\epsilon = 1.017$, $\eta = 0.4$, which correspond to $(\alpha,\beta) = (2.1663,0)$ for the CGLE (i.e., in subdomain IV in Fig. 1); (b) $\epsilon = 1.67$, $\eta = 0.2$, which correspond to $(\alpha,\beta) = (-0.4046,0)$ for the CGLE (i.e., in subdomain II in Fig. 1). $D(u/x)_{PS}$ [here, correspondingly, $D(u/x) = \partial_x u\partial_y v - \partial_y u\partial_x v$] is calculated, and $D(u/x)_{PS} > 0$ remains unchanged as time passes. That is, the topological charge W is conserved during the transition.

types of spirals in the CGLE while they have the same kind of spiral in the RD systems. As a case in point, we would like to study the FHN model. We can see from Fig. 10 that the original OPS in the FHN model will change its state to IPS after the system parameters have been changed suitably. At the same time, we also examine the topological charge and find that it is conserved. And during the spiral transition, we also find that, similar to the case of the CGLE, the chiralities are not conserved, and Eqs. (5) and (7) are satisfied well (see Table IV). In fact, the similar transition in the FHN model can also be observed if we set IPS as the original state in turn.

In addition, we also study the spiral transitions in the nonuniform Oregonator model [34] and the modified standard model [35]. After that, we further investigate the chiralities and their transitions in such cases. Finally, we find that the topological charges are conserved while the chiralities are not conserved, and Eqs. (5)–(7) can also work as well as in all of the above cases.

TABLE IV. The chirality transition in the FHN model.

Curl	Rotation	Propagation	Topological charge	FHN
$C = -1$	$R = -1$	$P = +1$	$W = +1$	Fig. 10(a)
$C = +1$	$R = -1$	$P = -1$	$W = +1$	Fig. 10(b)

IV. CONCLUSION

In summary, we have systemically studied the chiralities of spiral waves and their transition characteristics in the CGLE, which includes all kinds of spirals in uniform active media as shown in Figs. 2 and 3. In fact, the relationships traditionally discussed between the chiralities themselves and also between them and the topological charges only work for some special cases of spirals, namely, the OPSs in uniform excitable media. In this study, we get the general relationships between the chiralities and between them and the topological charges for various kinds of spiral waves. In addition, this study shows that the topological charges are conserved while the chiralities are not conserved during different kinds of spiral transitions. And in the process of the transitions, the general relationships both between the chiralities and between them and the topological charges still work effectively. We further find the above obtained results in the CGLE also serve well in some other models, such as the FHN model, the nonuniform Oregonator model, the modified standard model, etc. This study thus provides general properties and a comprehensive description for the chiralities of spiral waves and their transitions.

[1] J. M. Davidenko, A. V. Pertsov, R. Salomonsz, W. Baxter, and J. Jalife, Nature (London) **355**, 349 (1992).

[2] S. Jakubith, H. H. Rotermund, W. Engel, A. von Oertzen, and G. Ertl, Phys. Rev. Lett. **65**, 3013 (1990).

[3] A. T. Winfree, Science **175**, 634 (1972).

[4] R. A. Gray, A. M. Pertsov, and J. Jalife, Nature (London) **392**, 75 (1998).

[5] F. X. Witkowski, L. J. Leon, P. A. Penkoske, W. R. Giles, M. L. Spano, W. L. Ditto, and A. T. Winfree, Nature (London) **392**, 78 (1998).

[6] S. Luther, F. H. Fenton, B. G. Kornreich, A. Squires, P. Bittihn, D. Hornung, M. Zabel, J. Flanders, A. Gladuli, L. Campoy, E. M. Cherry, G. Luther, G. Hasenfuss, V. I. Krinsky, A. Pumir, R. F. Gilmour, Jr., and E. Bodenschatz, Nature (London) **475**, 235 (2011).

[7] S. Alonso, F. Sagués, and A. S. Mikhailov, Science **299**, 1722 (2003).

[8] H. Zhang, Z. J. Cao, N. J. Wu, H. P. Ying, and G. Hu, Phys. Rev. Lett. **94**, 188301 (2005).

[9] E. M. Cherry and F. H. Fenton, New J. Phys. **10**, 125016 (2008).

[10] A. T. Winfree, *When Time Breaks Down* (Princeton University Press, Princeton, NJ, 1987).

[11] V. S. Zykov, *Simulation of Wave Processes in Excitable Media* (Manchester University Press, Manchester, 1987).

[12] J. P. Keener and J. J. Tyson, SIAM Rev. **34**, 1 (1992).

[13] A. T. Winfree, Nature (London) **371**, 233 (1994).

[14] H. Zhang, B. B. Hu, B. W. Li, and Y. S. Duan, Chin. Phys. Lett. **24**, 1618 (2007).

[15] V. K. Vanag and I. R. Epstein, Science **294**, 835 (2001).

[16] X. Shao, Y. B. Wu, J. Z. Zhang, H. L. Wang, and Q. Ouyang, Phys. Rev. Lett. **100**, 198304 (2008).

[17] H. Skødt and P. G. Sørensen, Phys. Rev. E **68**, 020902(R) (2003).

[18] R. Straube, S. Vermeer, E. M. Nicola, and T. Mair, Biophys. J. **99**, L04 (2010).

[19] X. J. Yuan, H. L. Wang, and Q. Ouyang, Phys. Rev. Lett. **106**, 188303 (2011).

[20] Y. F. Gong and D. J. Christini, Phys. Rev. Lett. **90**, 088302 (2003).

[21] L. Brusch, E. M. Nicola, and M. Bär, Phys. Rev. Lett. **92**, 089801 (2004).

[22] E. M. Nicola, L. Brusch, and M. Bär, J. Phys. Chem. B **108**, 14733 (2004).

[23] H. X. Hu, L. Ji, and Q. S. Li, J. Chem. Phys. **128**, 044904 (2008).

[24] X. Gao, X. Feng, M. C. Cai, B. W. Li, H. P. Ying, and H. Zhang, Phys. Rev. E **85**, 016213 (2012).

[25] I. V. Biktasheva and V. N. Biktashev, Phys. Rev. E **67**, 026221 (2003).

[26] H. L. Wang and Q. Ouyang, Chin. Phys. Lett. **21**, 1437 (2004).

[27] Q. Wang, Q. Y. Gao, H. P. Lv, and Z. G. Zheng, Europhys. Lett. **92**, 50005 (2010).

[28] I. S. Aranson and L. Kramer, Rev. Mod. Phys. **74**, 99 (2002).

[29] M. C. Cross and P. C. Hohenberg, Rev. Mod. Phys. **65**, 851 (1993).

[30] X. Y. He, H. Zhang, B. B. Hu, Z. J. Cao, B. Zheng, and G. Hu, New J. Phys. **9**, 66 (2007).

[31] N. D. Mermin, Rev. Mod. Phys. **51**, 591 (1979).

[32] Y. S. Duan and H. Zhang, Phys. Rev. E **60**, 2568 (1999); Y. S. Duan and M. L. Ge, Scientia Sinica **11**, 1072 (1979).

[33] W. Jahnke, W. E. Skaggs, and A. T. Winfree, J. Phys. Chem. **93**, 740 (1989).

[34] B. W. Li, H. Zhang, H. P. Ying, W. Q. Chen, and G. Hu, Phys. Rev. E **77**, 056207 (2008).

[35] C. Wang, C. X. Zhang, and Q. Ouyang, Phys. Rev. E **74**, 036208 (2006).